

# Shear-induced criticality near a liquid-solid transition of colloidal suspensions

Masamichi J. Miyama<sup>1</sup> and Shin-ichi Sasa<sup>1</sup>

<sup>1</sup>*Department of Pure and Applied Sciences, University of Tokyo, Komaba, Meguro-ku, Tokyo 153-8902, Japan*

(Dated: February 23, 2024)

We investigate colloidal suspensions under shear flow through numerical experiments. By measuring the time-correlation function of a bond-orientational order parameter, we find a divergent time scale near a transition point from a disordered fluid phase to an ordered fluid phase, where the order is characterized by a nonzero value of the bond-orientational order parameter. We also present a phase diagram in the  $(\rho, \dot{\gamma}^{\text{ex}})$  plane, where  $\rho$  is the density of the colloidal particles and  $\dot{\gamma}^{\text{ex}}$  is the shear rate of the solvent. The transition line in the phase diagram terminates at the equilibrium transition point, while a critical region near the transition line vanishes continuously as  $\dot{\gamma}^{\text{ex}} \rightarrow 0$ .

PACS numbers: 64.60.Cn, 83.10.Mj, 83.50.Ax, 83.60.Rs

*Introduction:* A crystal phase is distinguished from a liquid phase by a translational and rotational symmetry breaking in space. Since there exists an order parameter associated with the symmetry-breaking, the nature of the transition to a crystal phase is rather different from that of gas-liquid transitions, although both are first-order transitions from the viewpoint of thermodynamics. In short, the transition to a crystal phase is classified as a symmetry-breaking first-order transition.

The correlation time of fluctuations does not diverge near symmetry-breaking first-order transitions. This is in sharp contrast to the case of a symmetry-breaking second-order transition, which exhibits a divergent time scale, as is observed in the case of decreasing temperature around a critical point of liquid-gas transitions. On the basis of standard understanding, in the present Letter, we argue that a divergent time scale of steady-state fluctuations may appear near an equilibrium crystallization (symmetry-breaking first-order transition) point when a non-equilibrium condition is imposed on the system.

Concretely, we study colloidal suspensions under shear flow through numerical experiments. Since the pioneering work by Ackerson and Clark [1], there have been extensive studies related to the crystallization of colloidal suspensions under shear flow [2–6]. In particular, a phase diagram was obtained by numerical experiments [2] and laboratory experiments [3], together with numerical realizations of crystal-liquid coexistence under shear flow [4]. In order to clarify the microscopic mechanism for the transition to a crystal, the kinetics of homogeneous nucleation under shear flow was also investigated [5]. However, to our knowledge, shear-induced criticality near an equilibrium crystallization point has never been reported, except for our preliminary observation [6].

In the present study, we focus on time scales associated with the relaxation from a bond-orientational ordered state in a disordered regime. We first note that the relaxation time, even in equilibrium cases, diverges near the melting point. We characterize the parameter dependence of the relaxation time quantitatively by measurement of the time series of a bond-orientational order

parameter. The result is well fitted by the Vogel-Fulcher law, which suggests the existence of a nucleation process of disordered fluid regions in a crystal state. However, since crystals do not appear spontaneously in the disordered phase, the divergent time scale has never been observed in steady state fluctuations. In contrast, in non-equilibrium systems under shear flow, the relaxation time exhibits a power-law divergence near a transition point to an ordered fluid, which suggests the existence of critical slowing down. The power-law divergent time scale is also observed in steady state fluctuations. We refer to this novel phenomenon as *shear-induced criticality near a liquid-solid transition*.

*Model:* We investigate  $N$  colloidal particles that are suspended in a solvent fluid confined to an  $L \times L \times L$  cubic box. We impose planar Couette flow on the solvent and choose the  $x$ -axis and the  $z$ -axis to be the directions of the shear velocity and the velocity gradient, respectively. Concretely, the velocity profile of the solvent is assumed to be given as  $(\dot{\gamma}^{\text{ex}}z, 0, 0)$ . We impose periodic boundary conditions along the  $x$ -axis and the  $y$ -axis and introduce two parallel walls so as to confine particles in the  $z$  direction.

Let  $\mathbf{r}_i$ ,  $i = 1, \dots, N$ , be the position of particle  $i$ . The potential energy of particles  $U(\{\mathbf{r}_j\}_{j=1}^N)$  consists of two parts,  $\sum_{i<j} U^{\text{LJ}}(|\mathbf{r}_i - \mathbf{r}_j|)$  and  $\sum_i U^{\text{wall}}(\mathbf{r}_i)$ . The former describes the interaction potential among particles, where  $U^{\text{LJ}}(r) = 4\epsilon((\sigma/r)^{12} - (\sigma/r)^6) - U_{\text{cutoff}}$  for  $r < r_c$  with cut-off length  $r_c$  and  $U_{\text{cutoff}} = 4\epsilon((\sigma/r_c)^{12} - (\sigma/r_c)^6)$ , while  $U^{\text{LJ}}(r) = 0$  otherwise.  $U^{\text{wall}}(\mathbf{r}_i)$  represents the wall potential and is given by  $U^{\text{wall}}(\mathbf{r}_i) = u^{\text{WCA}}(r^* - L/2 \pm z_i)$  for  $L/2 \pm z_i < r^*$  with the Weeks-Chandler-Andersen potential  $u^{\text{WCA}}$  [7], while  $U^{\text{wall}}(\mathbf{r}_i) = 0$  otherwise.

We define momentum of the  $i$ -th particle relative to the shear flow as  $\mathbf{p}_i(t) \equiv m\dot{\mathbf{r}}_i(t) - m\dot{\gamma}^{\text{ex}}z_i(t)\mathbf{e}_x$ , where  $m$  is the mass of a single particle. We then assume the equation of motion for the particles as

$$\frac{d\mathbf{p}_i}{dt} = -\frac{\partial U(\{\mathbf{r}_j\}_{j=1}^N)}{\partial \mathbf{r}_i} - \zeta \frac{\mathbf{p}_i}{m} + \boldsymbol{\xi}_i(t), \quad (1)$$

where  $\xi_i = (\xi_i^x, \xi_i^y, \xi_i^z)$  represents thermal noise satisfying  $\langle \xi_i^\alpha(t) \xi_j^\beta(t') \rangle = 2\zeta k_B T \delta_{ij} \delta^{\alpha\beta} \delta(t-t')$ ,  $k_B$  is the Boltzmann constant,  $T$  is the temperature of the solvent, and  $\zeta$  is the friction coefficient. The superscripts  $\alpha$  and  $\beta$  represent Cartesian components. (See Ref. [8].)

In numerical simulations, all the quantities are converted to dimensionless forms by setting  $m = \sigma = \epsilon = 1$ . We fix  $T = 1.5$ ,  $\zeta/k_B T = 1$ ,  $N = 1024$ ,  $r_c = 2.5\sigma$ , and  $r^* = 0.5\sigma$ , and treat  $\rho$  and  $\dot{\gamma}^{\text{ex}}$  as control parameters. We discretize (1) according to the reversible system propagator algorithm method [9] with time step  $\Delta t = 1/256$ . In the present Letter,  $\langle \dots \rangle$  represents the statistical average in steady states.

*Order parameters:* We define an order parameter that characterizes a rotational symmetry breaking [10, 11]. Using the Delaunay triangular decomposition [12] on a particle configuration, we determine neighboring particles for a given particle  $i$ . The collection of edges that extend from  $\mathbf{r}_i$  in the Delaunay triangular is denoted by  $(\mathbf{r}_{ij})_{j=1}^{n_B(i)}$ , where  $n_B(i)$  represents the number of neighbors of particle  $i$ . From this collection, we define a 13-dimensional vector  $\mathbf{q}_6(i) = (q_{6,-6}(i), \dots, q_{6,m}(i), \dots, q_{6,6}(i))$  as

$$q_{6,m}(i) = \frac{1}{n_B(i)} \sum_{j=1}^{n_B(i)} Y_{6,m} \left( \frac{\mathbf{r}_{ij}}{|\mathbf{r}_{ij}|} \right), \quad (2)$$

where  $Y_{6m}$  is the spherical harmonics function of degree six. Then, the bond-orientational order is qualified by

$$\bar{q}_{6,m} = \frac{1}{N} \sum_{i=1}^N q_{6,m}(i). \quad (3)$$

Here,  $\langle \bar{q}_{6,m} \rangle = 0$  if the rotational symmetry is not broken, while  $\langle \bar{q}_{6,m} \rangle \neq 0$  in the thermodynamic limit  $N \rightarrow \infty$  when the bond-orientational order emerges. In order to detect symmetry-breaking, it is convenient to measure the magnitude of the vector  $\bar{\mathbf{q}}_{6,m}$ . Following the standard convention, we define

$$Q_6 \equiv \left\langle \left( \frac{4\pi}{13} \sum_{m=-6}^6 \bar{q}_{6,m} \bar{q}_{6,m}^* \right)^{1/2} \right\rangle. \quad (4)$$

Note that  $Q_6 \simeq O(1/\sqrt{N})$  in the disordered phase, while  $Q_6 \simeq O(1)$  in the ordered phase, when  $N \rightarrow \infty$ .

On the left-hand side of Fig. 1, we show  $Q_6$  as a function of  $\rho$  for several values of  $\dot{\gamma}^{\text{ex}}$ . The figure indicates the existence of an ordered state with  $Q_6 \simeq O(1)$  in a high-density regime for each  $\dot{\gamma}^{\text{ex}}$ . In particular, the transition to the ordered phase is quite sharp when  $\dot{\gamma}^{\text{ex}} = 0$ , while the transition width becomes wider as  $\dot{\gamma}^{\text{ex}}$  is increased. For a tentative value of the transition point, we define  $\rho_q$  as the density such that  $Q_6 = 0.2$ . We display  $\rho_q$  as a function of  $\dot{\gamma}^{\text{ex}}$  in the right-hand side of Fig. 1. More precise determination of the functional forms of  $Q_6$  will

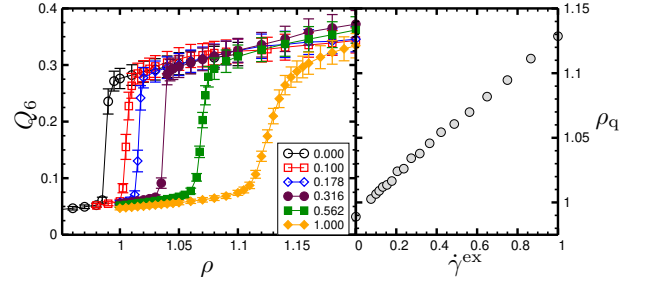


FIG. 1: (Color online) Left:  $Q_6$  as a function of  $\rho$  for several values of  $\dot{\gamma}^{\text{ex}}$ . Right:  $\rho_q$  as a function of  $\dot{\gamma}^{\text{ex}}$ .

be obtained by investigating larger systems. Note that in the thermodynamic limit without shear flow, non-zero  $Q_6$  emerges continuously for a density at which a crystal can coexist with a liquid. When we ignore the coexistence phase,  $Q_6$  exhibits a discontinuous transition, which is observed for the system under constant pressure. In the present Letter, putting aside phenomena associated with the coexistence phase, we focus on the question of how the nature of the symmetry-breaking discontinuous-transition is modified by the influence of shear flow.

In the equilibrium case, the ordered phase corresponds to a crystal. However, in the non-equilibrium cases, since the shear flow drives particles, particles may flow even in the ordered phase with  $Q_6 \neq 0$ . We then measure the  $x$ -component of the velocity averaged over a region with an interval  $[z + 0.5, z - 0.5]$  in the  $z$  direction, which is denoted by  $\bar{v}(z)$ . Examples of  $\bar{v}(z)$  for several values of  $\dot{\gamma}^{\text{ex}}$  with  $\rho = 1.1$  fixed are shown in the inset of Fig. 2. We then determine the shear rate  $\dot{\gamma}$  of particles by fitting the slope of the velocity profile  $\bar{v}(z)$  in the region  $-1.5 < z < 1.5$ . The obtained shear rates  $\dot{\gamma}$  are plotted for  $\dot{\gamma}^{\text{ex}}$  in Fig. 2. Although the flow might cease at some value of  $\dot{\gamma}^{\text{ex}}$ , the determination as to whether the cross-over is actually singular is a delicate problem. (See Ref. [14] for a related discussion.) For any case, the cross-over points are located at a higher density than  $\rho_q$  when  $\dot{\gamma}^{\text{ex}} > 0$ . (See Fig. 3.) Therefore, as we are concerned with behaviors near the transition point at which the order parameter  $Q_6 \simeq O(1)$  appears, we may assume that an ordered fluid is observed in the ordered phase in the non-equilibrium cases.

*Transition to the ordered fluid:* Next, we characterize the nature of the transition to the ordered phase. First, in order to observe a clear difference between the equilibrium and non-equilibrium cases, we measure the relaxation time  $\tau_{\text{rel}}$  at which  $Q_6$  reaches a value of 0.05, starting from a crystal state, which  $Q_6 \approx 0.35$ . Note that  $\tau_{\text{rel}}$  can be measured only in the disordered phase. In Fig. 4, we show  $\tau_{\text{rel}}$  as a function of  $\rho$  for several values of  $\dot{\gamma}^{\text{ex}}$ , where we set the maximum waiting time to  $\tau = 10000$ . The results indicate the existence of a charac-

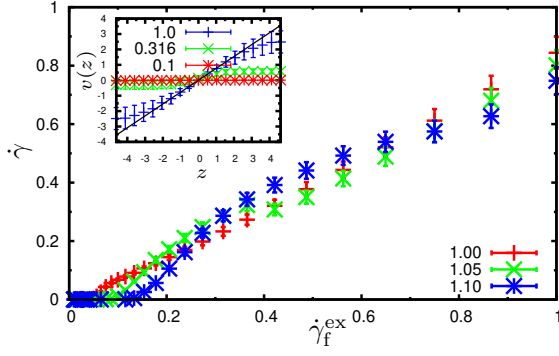


FIG. 2: (Color online) Shear rate of particle flow as a function of  $\dot{\gamma}^{\text{ex}}$  for several values of  $\rho$ . Each point is obtained from the velocity profiles  $\bar{v}(z)$ . Examples of velocity profiles for different  $\dot{\gamma}^{\text{ex}}$  with  $\rho = 1.1$  fixed are shown in the inset.

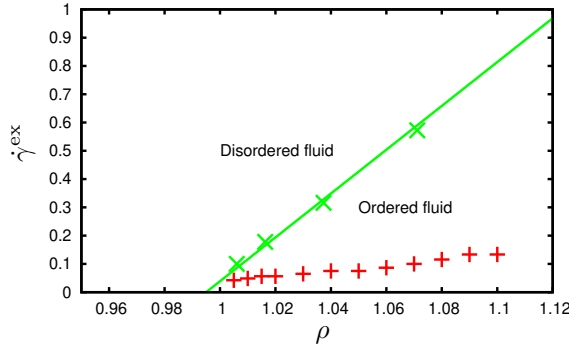


FIG. 3: (Color online) Phase diagram in the  $(\rho, \dot{\gamma}^{\text{ex}})$  plane. The green and cross symbols represent the transition line  $\rho = \rho_q(\dot{\gamma}^{\text{ex}})$  between the disordered fluid phase and the ordered fluid phase. The parameter values for realizing  $\dot{\gamma} = 10^{-3}$ , below which flow appears to cease, are also plotted as red plus symbols.

teristic density  $\rho_d$  at which the relaxation time diverges for each value of  $\dot{\gamma}^{\text{ex}}$ .

Let us determine the functional form of  $\tau_{\text{rel}}$  with the value of  $\rho_d$ . First, as shown in the inset of Fig. 5,  $\tau_{\text{rel}}$  for the equilibrium case is well fitted by the Vogel-Fulcher law

$$\tau_{\text{rel}} \simeq \tau_0 \exp\left(\frac{A}{\rho_d - \rho}\right). \quad (5)$$

A phenomenological argument may be developed for the nucleation of a disordered domain, by which (5) may be understood. (See for example Ref. [13] for a demonstration of a  $q$ -states Potts model.) In contrast, Fig. 5 indicates that  $\tau_{\text{rel}}$  for the systems under shear flow follows a power-law form

$$\tau_{\text{rel}} \simeq B(\dot{\gamma}^{\text{ex}})(\rho_d(\dot{\gamma}^{\text{ex}}) - \rho)^{-\zeta}, \quad (6)$$

where  $\zeta \simeq 1.6$ . This suggests that the divergent behavior does not originate from the nucleation of disordered regions but may be related to critical slowing down. Note

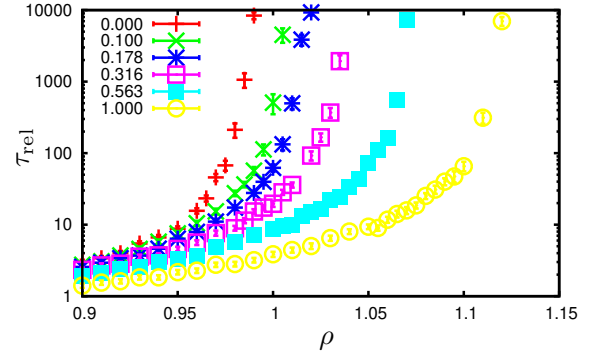


FIG. 4: (Color online) Relaxation time  $\tau_{\text{rel}}$  as a function of density  $\rho$  for several values of  $\dot{\gamma}^{\text{ex}}$ .

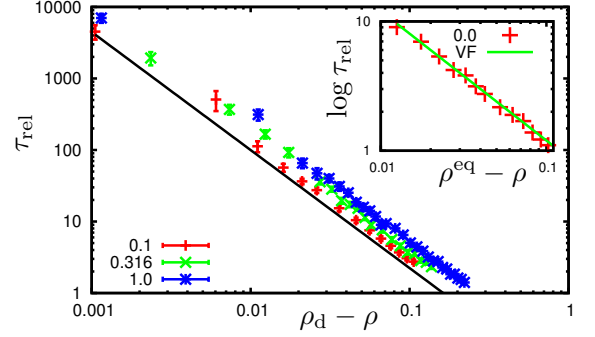


FIG. 5: (Color online) Fitting of functional forms of  $\tau_{\text{rel}}$  versus  $\rho_d - \rho$  with a log-log plot for  $\dot{\gamma}^{\text{ex}} = 0.1, 0.316$ , and  $1.0$ .  $\rho_d$  is a fitting parameter, the value of which is estimated as  $1.006, 1.037$ , and  $1.121$ , respectively. The guide line represents (6) with  $\zeta = 1.6$ . Inset:  $\log \tau_{\text{rel}}$  versus  $\rho_d - \rho$  with a log-log plot for  $\dot{\gamma}^{\text{ex}} = 0$ . The guide line represents (5) with  $A = 0.1$  and  $\rho_d = 1.003$ .

that the pre-factor  $B$  in (6) depends slightly on  $\dot{\gamma}^{\text{ex}}$  in the form  $B \simeq (\dot{\gamma}^{\text{ex}})^{0.3}$ , as shown in the inset of Fig. 6. Let  $\rho_w(\dot{\gamma}^{\text{ex}})$  be a typical width of the power-law region for  $\dot{\gamma}^{\text{ex}}$ . Then, on the basis of the dimensional analysis, it is expected that

$$\dot{\gamma}^{\text{ex}} \tau_{\text{rel}} \simeq \left( \frac{\rho_d(\dot{\gamma}^{\text{ex}}) - \rho}{\rho_w} \right)^{-\zeta}. \quad (7)$$

By assuming  $\rho_w \simeq (\dot{\gamma}^{\text{ex}})^\chi$  in (7), we obtain  $B \simeq (\dot{\gamma}^{\text{ex}})^{\chi\zeta-1}$ , which leads to  $\chi \simeq 1.3/1.6 > 0$ . This means that a critical region for the system with finite  $\dot{\gamma}^{\text{ex}}$  becomes narrower for smaller  $\dot{\gamma}^{\text{ex}}$  and vanishes in the equilibrium system. See the schematic phase diagram in Fig. 6.

We now note that such a divergent time scale is never observed in the stationary state of the equilibrium system. In order to confirm this explicitly, we measure the time correlation function defined by

$$C(t) = \sum_{m=-6}^6 [\langle \bar{q}_{6,m}(t_0) \bar{q}_{6,m}^*(t_0 + t) \rangle - \langle \bar{q}_{6,m} \rangle^2]. \quad (8)$$

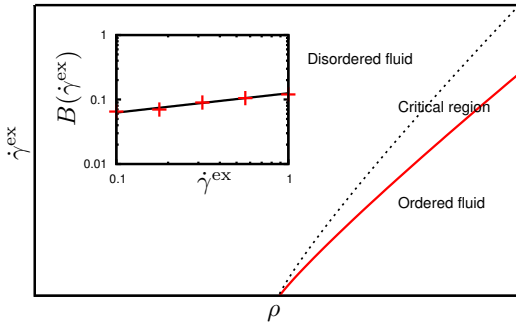


FIG. 6: (Color online) Schematic phase diagram with the critical region in the  $(\rho-\dot{\gamma}^{\text{ex}})$  plane. Inset:  $B(\dot{\gamma}^{\text{ex}})$  as a function of  $\dot{\gamma}^{\text{ex}}$ . The guide line represents a power-law function with exponent 0.3.

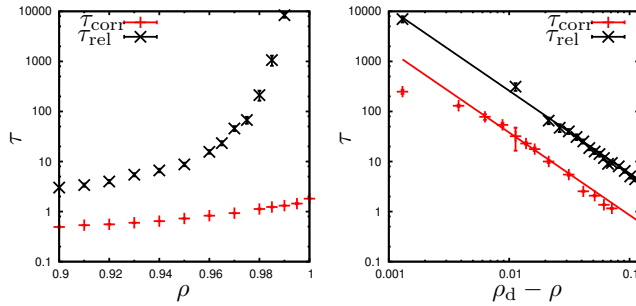


FIG. 7: (Color online) Correlation time  $\tau_{\text{corr}}$  in steady states as a function of  $\rho$ . The melting time  $\tau_{\text{rel}}$  is also superimposed for comparison. (Left:)  $\dot{\gamma}^{\text{ex}} = 0$ , and (Right:)  $\dot{\gamma}^{\text{ex}} = 1.0$ .

We determine the correlation time  $\tau_c$  from the fitting of the exponential decay rate of  $C(t)$ . On the left-hand side of Fig. 7,  $\tau_c$  is shown as a function of  $\rho$  in the disordered regime. Indeed, the correlation time does not diverge. For reference, we superimpose the data of the relaxation time  $\tau_{\text{rel}}$ . In contrast to the equilibrium case, as shown in the right-hand side of Fig. 7, the correlation time in the system under shear flow diverges in a manner similar to  $\tau_{\text{rel}}$ . These results indicate that the symmetry-breaking transition to the ordered fluid accompanies a critical phenomenon. This is the main claim of the present Letter.

*Concluding remarks:* Before ending this Letter, we address three considerations. First, we conjecture that the fluctuation of  $q_6$  possesses a divergent length scale. By investigating the manner of divergences of several quantities for systems of different sizes, the universality class for this phenomenon may be determined.

Second, with regard to the universality problem, we are also interested in a simple mathematical model in the same universality class. For example, it might be possible to propose a model describing a stochastic time evolution

of the coarse-grained order parameter field. The first problem in this direction is to derive the value of  $\zeta$  using a phenomenological argument.

Finally, in all of the arguments presented above, the coexistence phase is ignored. In order to extract more precise results, it might be better to investigate systems under constant pressure. A study of such systems of larger sizes will be performed in the future.

In summary, we have investigated colloidal suspensions under shear flow. We have found that the critical transition line starts from the liquid-solid transition point in the equilibrium system without shear flow. This novel phenomenon, referred to as shear-induced criticality, will be investigated from several viewpoints.

We thank M. Kobayashi for discussions on the role of the order parameters  $q_{6,m}$ . The present study was supported by grants from the Ministry of Education, Culture, Sports, Science, and Technology of Japan, Nos. 21015005 and 22340109, and by a Grant-in-Aid for JSPS Fellows (DC2), 21-10700, 2009.

- 
- [1] B. J. Ackerson and N. A. Clark, *Physica A* **110**, 221 (1983); *Phys. Rev. A* **30**, 906 (1984).
  - [2] S. Butler and P. Harrowell, *J. Chem. Phys.* **103**, 4653 (1995); *J. Chem. Phys.* **105**, 605 (1996).
  - [3] P. Holmqvist, M. P. Lettinga, J. Buitenhuis, and J. K. G. Dhont, *Langmuir* **21**, 10976 (2005).
  - [4] S. Butler and P. Harrowell, *Nature* **415**, 1008 (2002); *J. Chem. Phys.* **118**, 4115 (2003); *Phys. Rev. E* **67**, 051503 (2003).
  - [5] R. Blaak, S. Auer, D. Frenkel, and H. Löwen, *Phys. Rev. Lett.* **93**, 068303 (2004).
  - [6] M. J. Miyama and S.-i. Sasa, *J. Phys.: Condens. Matter* **20**, 035104 (2008).
  - [7] J. D. Weeks, D. Chandler, and H. C. Andersen, *J. Chem. Phys.* **54**, 5273 (1971).
  - [8] M. G. McPhie, P. J. Daivis, I. K. Snook, J. Ennis, and D. J. Evans, *Physica A* **299**, 412 (2001).
  - [9] M. Tuckerman, B. J. Berne, and G. J. Martyna, *J. Chem. Phys.* **97**, 1990 (1992); G. Bussi and M. Parrinello, *Phys. Rev. E* **75**, 056707 (2007).
  - [10] P. J. Steinhardt, D. R. Nelson, and M. Ronchetti, *Phys. Rev. B* **28**, 784 (1983); J. S. van Duijneveldt and D. Frenkel, *J. Chem. Phys.* **96**, 4655 (1992).
  - [11] U. Gasser, E. R. Weeks, A. Schofield, P. N. Pusey, and D. A. Weitz, *Science* **292**, 258 (2001); J. Hernández-Guzmán, and E. R. Weeks, *PNAS* **106**, 15198 (2009).
  - [12] D. C. Rapaport, *The Art of Molecular Dynamics Simulation 2nd Edition* (Cambridge University Press, 2004).
  - [13] F. Krzakala and L. Zdeborová, arXiv:1006.2480 (2010).
  - [14] F. Sausset, G. Biroli, and J. Kurchan, *J. Stat. Phys.* **140**, 718 (2010).